



Localized neighborhood species mingling is correlated with individual tree size inequality in natural forests in South China

Hong-Xiang Wang¹ · Shao-Xian Huang¹ · Shu-Sheng Zhang² · Hui Peng³ · Kun-Fang Cao¹

Received: 7 June 2021 / Accepted: 22 October 2021 / Published online: 28 December 2021
© INRAE and Springer-Verlag France SAS, part of Springer Nature 2021

Abstract

• **Key message** We identified the significant spatial relationships between tree species mingling and size inequality in various species-rich natural forests in South China. Forest communities with low species mingling, or segregation of heterospecific trees, exhibited increased segregation of trees with dissimilar sizes. Large trees were more likely to be associated with high species mingling, and variation in neighboring tree sizes would also increase neighborhood species diversity.

• **Context** Numerous hypotheses such as Janzen–Connell and herd immunity effects have been proposed to explain the coexistence of diverse species in plant communities. However, these mechanisms for maintaining diversity have been studied primarily through the lens of species diversity, whereas tree size diversity or relationships between size and species diversity resulting from local interactions have rarely been investigated.

• **Aims** We aimed to identify relationships between spatial species mingling and tree size inequality using extensive plot data from species-rich forest ecosystems.

• **Methods** We applied neighborhood-based methods and explored relationships between spatial species mingling and size inequality indices in 22 large forest plots (30 ha in total) in subtropical and tropical China.

• **Results** Forest communities with low species mingling, or segregation of heterospecific trees, exhibited increased segregation of trees with dissimilar sizes. In most plots, large trees (e.g., dbh > 30 cm) were extensively associated with high species mingling, and individual-tree neighborhood species and size diversity were closely correlated.

• **Conclusion** Our findings suggest that both the spatial patterns of conspecific dispersal and neighborhood interactions play an important role in determining the spatial patterns of tree size and species diversity and eventually in shaping the structure of forest communities.

Keywords Forest structure diversity · Intraspecific clustering · Janzen–Connell · Large trees · Size inequality · Species mingling

Handling Editor: Andreas Bolte

✉ Kun-Fang Cao
kunfangcao@gxu.edu.cn

Hong-Xiang Wang
wanghongxiang168@126.com

Shao-Xian Huang
huangshaoxian0211@163.com

Shu-Sheng Zhang
548708934@qq.com

Hui Peng
ericztu@vip.qq.com

¹ College of Forestry, Guangxi University, Nanning 530004, China

² Wuyanling National Natural Reserve Management Bureau, Wenzhou 325000, Zhejiang, China

³ Fengyangshan National Nature Reserve, Longquan 323700, Zhejiang, China

1 Introduction

Exploring the mechanisms that maintain the coexistence of diverse species in plant communities has long been a central objective of community ecology (Huston 1979; Chesson 2000; Levine et al. 2017). Localized tree interactions are fundamental factors that determine growth, survival, and competition stress of individual trees and ultimately influence the ontogenesis of forest community spatial structure diversity (Brown et al. 1995; Wright 2002; Armas and Pugnaire 2005; Pretzsch 2009). As one of the most well-known and extensively studied tree interaction effects that maintain plant species diversity, the Janzen and Connell (JC) hypothesis (Connell 1970; Janzen 1970) describes local effects that impair the performance of conspecific neighbors in forest communities due to host-specific pathogens, herbivores, seed predators, and intraspecific competition. Studies have shown that strong JC effects can be understood as *conspecific negative density dependence* (LaManna et al. 2017; Germany et al. 2019), in which the survival probability of juvenile trees growing in high-density conspecific patches is reduced compared to the ones growing in heterospecific patches. In addition, according to the *herd protection hypothesis* (Wills et al. 1997), which is considered an extension of the JC hypothesis (Raventós et al. 2010), heterospecific neighbors are exposed to fewer encounters with species-specific pests and pathogens and thus have greater fitness and can be considered “protected,” non-susceptible neighbors in a matrix of susceptible hosts (Peters 2003). Extensive studies have shown that both JC and herd protection effects are well-documented driving factors that maintain local species diversity in plant communities (Wright 2002; Zhu et al. 2010; Bagchi et al. 2011; Shuai et al. 2014). To date, however, the processes involved in maintaining tree diversity have been studied primarily through the lens of species diversity, whereas tree size diversity (also referred to as size inequality or size hierarchy) or relationships between tree size and species diversity resulting from these local interactions have rarely been investigated (Pommerening et al. 2020; Wang et al. 2020).

Spatial clustering of conspecific trees has been documented in various natural forest types (Condit et al. 2000; Perry et al. 2008), and the causes have generally been attributed to dispersal limitations and environmental filtering (Seidler and Plotkin 2006; Shen et al. 2013). Spatial aggregation of conspecifics results in low species mingling of individuals in their immediate neighborhood, and due to tree size distribution of the same species is often limited within a range in natural forests (Pommerening et al. 2020; Wang et al. 2020) conspecific clustering would also lead to neighborhood size equality or spatial aggregation of similar

tree sizes. According to the JC and herd protection effects, the emergence of conspecific cohorts increases the significance of intraspecific interactions, leading to the selective exclusion of neighboring conspecifics and hence increasing distances between conspecifics as trees move from early- to late-growth stages (Sterner et al. 1986; Zhu et al. 2010; Yao et al. 2016). Eventually, heterospecific neighbors can occupy or benefit from the released space and resources caused by these processes, which therefore can effectively enhance both localized species mingling and size inequality of the large individuals survived from conspecific density-dependent mortality. Additionally, as trees grow to larger sizes, they often have a greater impact on the dynamics of neighboring trees; hence, heterospecific neighbors surrounding the large-sized trees should have higher survival chances when intraspecific interaction is strong. As succession progresses, the above effects strengthen species and size replacement and, hence, up to a point increase both localized neighborhood species and size diversity (Pommerening and Grabarnik 2019).

Studying the resulting diversity effects for species and size, Pommerening and Uria-Diez (2017) and Wang et al. (2018) found that there is often a tendency for large trees to be surrounded by smaller, heterospecific nearest neighbors and that localized tree species mingling and size inequality are positively correlated. As a spatial extension of JC and herd protection effects, the authors referred to this phenomenon as the *mingling-size hypothesis*.

Understanding the link between structure, processes, and forest dynamics provides basic theoretical and practical guidance for sustainable forest management, particularly for conservation (Pretzsch 2009). Because dissimilarities in tree species and sizes are key determinants of forest stand properties and tree diversity (Liang et al. 2007; Gadow et al. 2012; Hui and Pommerening 2014), exploring mingling-size effects is crucial to understanding forest dynamics and the evolution of tree diversity at local scale. Although mingling-size effects have been reported in several forests, evidence has mainly come from managed or unmanaged temperate forests (see Pommerening and Uria-Diez 2017; Wang et al. 2018). The prevalence and strength of mingling-size effects in plant communities should thus be systematically explored in other, more diverse natural forest ecosystems in different climate zones. Of particular interest are subtropical and tropical forests that have the highest tree diversity in forest ecosystems worldwide. Studies have demonstrated that, compared to temperate forests, where species diversity is relatively low, the strength of conspecific biotic interactions is stronger in subtropical and tropical forests due to a large number of specialized enemies (Dyer et al. 2007; Forister et al. 2015). As a consequence, positive correlations between

spatial species mingling and size inequality caused by such strong biotic effects, as expected, may be identified more readily in warm climate zones.

In order to improve our understanding of how intra- and inter-specific plant interactions shape spatial diversity patterns, the present study aimed to identify spatial relationships between tree size inequality and species diversity using extensive plot data from species-rich subtropical and tropical forest ecosystems. We first compared the stand structure characteristics of the studied forest plots, and investigated the correlations between species and size diversity patterns among forest communities. Secondly, for each forest plot, we identified the relationships between individual tree size inequality and localized species mingling in order to determine whether large trees are more likely to be surrounded by heterospecific neighbors as expected, and to investigate whether variation in neighboring tree sizes would also increase species mingling.

2 Material and methods

2.1 Study site and tree data

Twenty-two plots were established in seven natural reserves located in different regions of South China, ranging from mid-subtropical to tropical monsoon climate zones (Fig. 1). All the forest plots are protected natural mixed forests comprising diverse species and represent a variety of forest types, such as evergreen broad-leaved forests, mid-subtropical evergreen broad-leaved and coniferous forests, mid-subtropical evergreen and deciduous broad-leaved mixed forests, and tropical monsoon rainforests. Among the studied plots, twenty-one 1-ha plots were established in six national natural reserves in different regions of Guangxi province, i.e., Shiwanshan, Jiuwanshan, Damingshan, Huaping, Dayaoshan, and Mulun Forest Reserve. Specifically, forest stands in the Mulun Forest Reserve are characterized by karst landscapes shaped by substantial limestone erosion, widespread

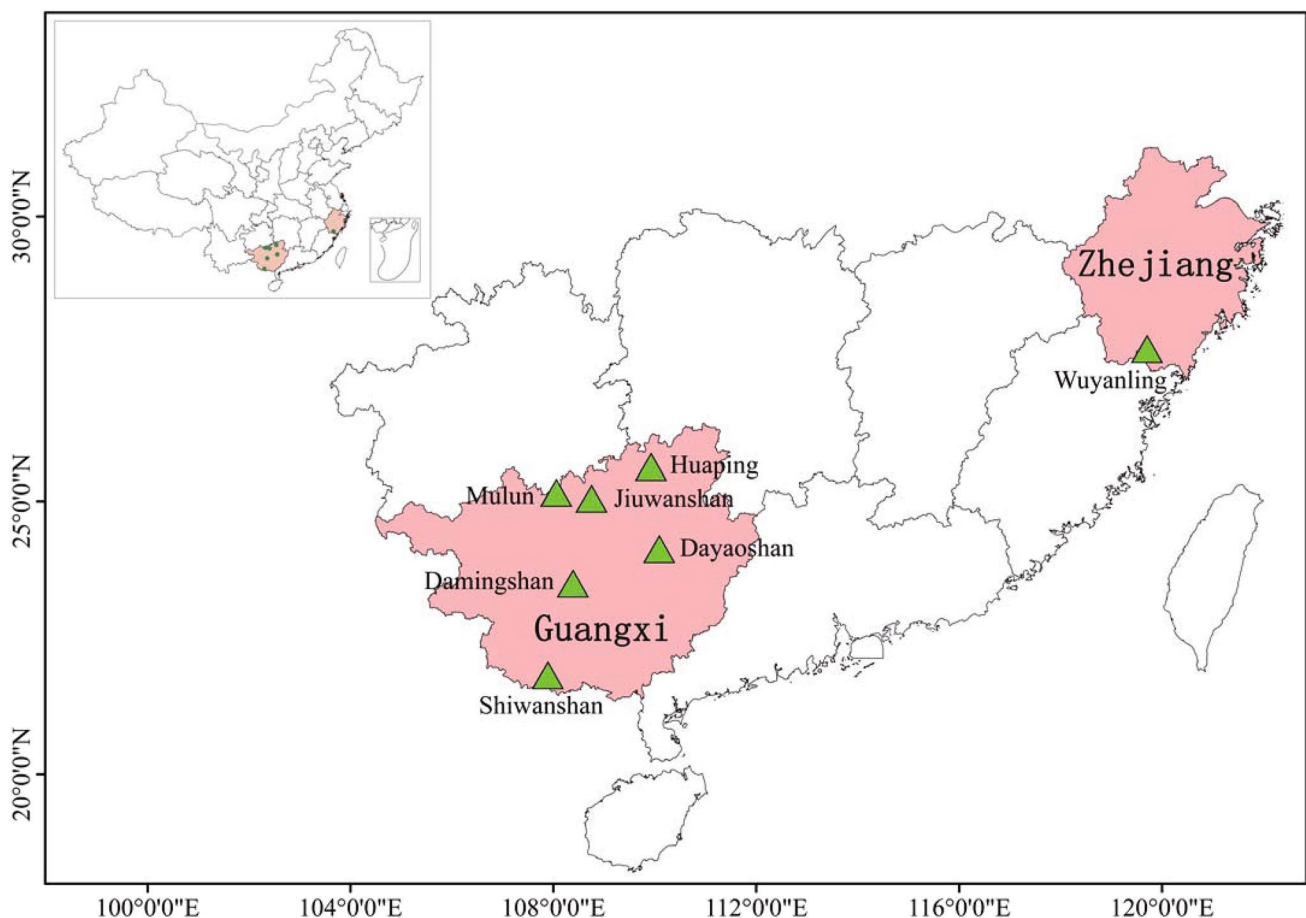


Fig. 1 The seven study sites, comprising 22 plots with a total area of 30 ha

exposed bedrock, and poor soil carrying capacity. One 9-ha plot is located in the Wuyanling National Natural Reserve in Zhejiang Province and is part of the mid-subtropical climate zone of southeast China. Basic information about the seven study sites is provided in Table 1.

For referring to each forest plot, we used abbreviations to denote each plot in the remainder of the text. Two or three letters were used to represent forest reserve names, and each individual plot belonging to a certain reserve was given a further letter to allow plot identification within each forest reserve. For example, we used Dys a to denote plot a in the Dayaoshan Forest Nature Reserve.

The Damingshan Forest Nature Reserve (Dms) is located in south-central Guangxi Province, in the transitional belt between the north and south subtropical climate zones. The Tropic of Cancer passes through its central part, and forests in this region primarily have a moist (southern) subtropical monsoon climate (Wen et al. 1998). Broad-leaved evergreen forests dominated by species of *Castanopsis fargesii* FRANCH., *Schima argentea* PRITZ. EX DIELS, *Rhododendron henryi* HANCE, *Castanopsis eyrei* (CHAMP.) TUTCH. are typical in this region. Two stands (Dms a and b) from this forest were included in this study.

The Dayaoshan Forest Nature Reserve (Dys) is located in the center of the eastern part of the arcuate mountain belt in Guangxi Province, which has a monsoon climate and is transitional between the southern subtropical and mid-subtropical zones. The climate is moderate, without extreme temperatures in winter or summer. This area mainly has coniferous and broadleaved mixed forests dominated by *Acanthopanax sinensis* HOO, *Castanopsis fabri* HANCE, *Rapanea neriifolia* (SIEB. ET ZUCC.) MEZ, and *Lindera metcalifiana* ALLEN among others. Four plots (Dys a–d) were established in this reserve.

The Huaping National Nature Reserve (Hp) is located in northeast Guangxi province, and forms a part of the Nanling Mountain range. The protected plant species in the reserve include *Cathaya argyrophylla* CHUN ET KUANG and other species unique to mid-subtropical broad-leaved forests. Forest types include subtropical mid-mountain deciduous broad-leaved mixed forests, dominated by species in the Fagaceae, Lauraceae, Theaceae, Hamameliaceae, Araliaceae, Magnoliaceae, and Symplocaceae families. Four forest stands (Hp a–d) were included in this study.

The Jiuwanshan National Nature Reserve (Jws) is situated in the northern part of Guangxi Province. The reserve is at the southern end of the Miaoling Mountains and the altitudes for most of the mountains are above 1,000 m. The climate type of the reserve is a mid-subtropical monsoon climate. Three stands (Jws a–c) were included in this study, representing typical mid-subtropical evergreen broad-leaved coniferous forests. The main tree species in this site include *Castanopsis hystrix* A. DC., *Lindera kwangtungensis* (LIU)

ALLEN, *Machilus chinensis* (CHAMP. EX BENTH.) HEMSL., and *Engelhardtia roxburghiana* WALL.

The Mulun National Nature Reserve (MI) is located in northwestern Guangxi Province, and belongs to the evergreen and deciduous broad-leaved forest of the limestone region in the mid-subtropical zone. The mixed-species forest ecosystem represents the largest extant karst forest in the world. Forest cover in this region reaches 94.18%, and vegetation is strongly influenced by a mid-subtropical monsoon climate. Three forest plots (MI a–c) were established in the reserve, representing typical natural, evergreen, and deciduous broad-leaved mixed forests of karst landform. The stands included in this research are mainly composed of *Pteroceltis tatarinowii* MAXIM., *Boniiodendron minus* (HEMSL.) T. CHEN, *Radermachera sinica* (HANCE) HEMSL., and *Tarenna depauperata* HUTCHINS.

The Shiwandashan National Nature Reserve (Sws) is situated in the southwestern part of Guangxi Province. The vegetation in this region is largely shaped by a northern tropical monsoon climate. Rainfall is particularly abundant at this site, as the southwest monsoon currents move from sea to land. The tropical monsoon forest is the climax forest vegetation under local climatic conditions. Species richness is distinctly high in this region and the main tree species are *Cinnamomum parthenoxylon* (JACK) MEISNER, *Engelhardtia roxburghiana* WALL., *Aporosa dioica* (ROXB.) MÜLL. ARG., and *Raphiolepis indica* (LINNAEUS) LINDLEY. Five stands, abbreviated as Sws a–e, were included in this study.

The Wuyanling National Nature Reserve (Wyl), located in Taishun County, Wenzhou City, is the largest natural reserve in Zhejiang Province. The reserve is located within the mid-subtropical climate zone and is influenced by the East Asian monsoon. The climate is characterized by four distinct seasons, with mild, wet springs and autumns; a hot, humid summer; and a short, dry period in winter. This area mainly has secondary evergreen broad-leaved forest dominated by *Vaccinium carlesii* DUNN, *Cyclobalanopsis stewardiana* (A. CAMUS) Y. C. HSU ET H. W. JEN, *Machilus litseifolia* S. K. LEE, and *Ilex rotunda* THUNBERG. One 9-ha forest monitoring plot was established in 2012 (Zhong et al. 2015) and was included in this study.

Data from the fully mapped plots included all live trees larger than 1 cm, and each individual tree was tagged, numbered, and mapped and their species and diameters at breast height (measured at 1.3 m above ground level; dbh) were recorded.

2.2 Tree species mingling and size inequality

Neighborhood-based indices which describe the relationships between an individual tree and its natural nearest neighbors according to Euclidean distance were used to characterize spatial patterns of tree species or sizes. Species

Table 1 Basic information for the seven study sites

Region	Number of plots	Latitude	Longitude	Altitude range (m)	Annual mean temperature (°C)	Mean temperature of warmest quarter (°C)	Mean temperature of coldest quarter (°C)	Annual precipitation (mm)	Climate type	Typical vegetation type
Dms	2	23°29'42"– 23°31'10"	108°23'11"– 108°26'27"	1166–1251	21.4	28.0	13.5	1600	Southern subtropical monsoon climate	Evergreen broad-leaved forests
Dys	4	23°58'8"– 24°8'43"	110°05'15"– 110°6'48"	478–1321	18.8	25.2	11.0	1690	Southern subtropical monsoon climate	Mixed coniferous and broadleaved forests
Hp	4	25°36'6"– 25°37'8"	109°54'12"– 109°55'31"	700–1600	18.6	26.7	9.4	1700	Mid-subtropical monsoon climate	Mid-mountain deciduous broad-leaved mixed forests
Jws	3	25°03'16"– 25°12'22"	108°40'18"– 108°45'6"	652–1347	19.7	27.5	10.8	1490	Mid-subtropical monsoon climate	Evergreen broad-leaved coniferous forests
MI	3	25°6'50"– 25°9'36"	107°57'30"– 108°03'29"	368–694	20.1	27.3	11.6	1424	Mid-subtropical monsoon climate	Evergreen and deciduous broad-leaved forests
Sws	5	21°50'31"– 21°51'58"	107°52'54"– 108°01'14"	340–655	22.1	27.9	14.9	2350	Tropical monsoon climate	Tropical monsoon rainforests
Wyl	1	27°42'10"– 27°42'20"	109°40'06"– 109°40'19"	869–1145	14.0	23.0	4.0	2200	Mid-subtropical monsoon climate	Evergreen broad-leaved forests

mingling index quantifies the proportion of the k nearest neighbors that have a species different from the species of a particular reference tree (Gadow and Fuldner 1993; Aguirre et al. 2003). The measure expresses the spatial extent of species mixing, as follows:

$$M_i^{(k)} = \frac{1}{k} \sum_{j=1}^k \mathbf{1}(\text{species}_i \neq \text{species}_j) \quad (1)$$

Here $\mathbf{1}()$ is an indicator function that returns the value of 1, if the condition in the brackets is fulfilled and 0 otherwise. Hence, the greater the value of $M_i^{(k)}$, the higher the local species diversity of a reference tree i .

For the calculation of $M_i^{(k)}$, different numbers, k , of neighboring trees (e.g., $k = 4$ or $k = 6$) can be used, and different neighbors imply that depending on tree density varying distances around a reference tree are considered. Since trees mostly interact with their immediate neighbors, and to avoid excessively short or large distances between an individual tree and its k th neighboring tree, we used an increasing number of k (4, 6, 8, and 10) to calculate mingling values with the aim that adequate sizes of local neighborhoods are considered.

We calculated size differentiation index ($T_i^{(k)}$) to measure the local neighborhood size inequality of individual trees (Gadow 1993). The index is defined as the mean of the ratio of smaller-sized and larger-sized plant characteristic m of the k nearest neighbors subtracted from one. Similar to the species mingling index, $T_i^{(k)}$ can be calculated for every individual plant i .

$$T_i^{(k)} = 1 - \frac{1}{k} \sum_{j=1}^k \frac{\min(m_i, m_j)}{\max(m_i, m_j)} \quad (2)$$

The value of $T_i^{(k)}$ increases with increasing average size difference between neighboring trees. Similar to species mingling, $k = 4, 6, 8,$ and 10 nearest-neighbor trees were used to quantify the size differentiation index and its value ranges from 0 to 1 regardless of the value of k . $T_i^{(k)} = 0$ implies that neighboring trees have equal size and 1 indicates the greatest possible difference between tree sizes.

In point process statistics, observed spatial measures are often compared with expected measures that, as a null hypothesis, represent spatial patterns with no correlation between plant locations and/or plant attributes (such as species or size). In order to study the difference between observed and expected species mingling and size differentiation, we also calculated the species and size segregation indices (Pommerening and Grabarnik 2019; Wang et al. 2020) in Eqs. (3) and (4), respectively.

$$\Psi^{(k)} = 1 - \frac{\overline{M}^{(k)}}{\text{EM}} \quad (3)$$

$$\Upsilon^{(k)} = 1 - \frac{\overline{T}^{(k)}}{\text{ET}} \quad (4)$$

Here $\overline{M}^{(k)}$ and $\overline{T}^{(k)}$ are mean community species mingling and size differentiation indices, respectively. EM and ET are the aforementioned expected values representing the independent spatial arrangement of tree species or size (see Pommerening and Grabarnik 2019, p. 132f. and 140f.). $\Psi^{(k)}$ and $\Upsilon^{(k)}$ have values between -1 and 1 ; a value of 0 means that plant species/sizes are independently dispersed without any spatial correlation; negative values tending towards -1 are obtained if the majority of trees attract neighbors of different species/sizes, while positive values with a maximum of 1 indicate an attraction of the same species or similar sizes (Pommerening et al. 2019, 2020).

As spatial size and species diversity are primary attributes of α -diversity at the community level (Pommerening and Grabarnik 2019), possible correlations between the mean spatial species mingling and size inequality of forest communities facilitate a better understanding of tree diversity maintenance mechanisms in the spatial context in forest ecosystems. We explored the correlations of mean community species and size inequality indices, i.e., species mingling/size differentiation indices and species/size segregation indices, across the studied forest communities. Strong positive correlations between spatial species mingling and size inequality imply that communities with different species mingled would also have high tree size diversity at the local scale.

2.3 Logistic regression

In order to quantify the relationships between species mingling and tree sizes, we applied logistic regression and modeled the probability of high species mingling as predicted by individual tree sizes (dbh) or local size diversity measured by size differentiation ($T_i^{(k)}$). We used diameter at breast height (dbh) as the size variable of trees, since dbh is the most commonly measured tree size variable. Similar to Pommerening and Uria-Diez (2017), we grouped species mingling values into two groups, i.e., low and high species mingling, and, thus, obtained a binary predicted variable. This binary variable can be used in a logistic model with dbh or $T_i^{(k)}$ as explanatory variables.

$$P_m = \frac{e^{\beta_1 \cdot x + \beta_0}}{1 + e^{\beta_1 \cdot x + \beta_0}} \quad (5)$$

where P_m denotes the probability of high mingling of individuals and x is the explanatory variable, i.e., tree size (dbh) or size differentiation ($T_i^{(k)}$). β_0 is the intercept term, and β_1 is the slope coefficient for a single input value x . Large slope values indicate a stronger dependence of the probability of

Table 2 Summary structure characteristics of the 22 observational natural forest plots. *dbh*, diameter at breast height; $\hat{M}^{(k)}$ and $\hat{T}^{(k)}$ —species mingling and size differentiation indices; and $\hat{\Psi}^{(k)}$ and $\hat{Y}^{(k)}$ —species segregation and size segregation indices. $k = 4$ was used to compute the nearest neighbor indices

Region	Plot	Plot size (m×m)	Density (trees ha ⁻¹)	Number of species	Max dbh (cm)	Basal area (m ² ha ⁻¹)	$\hat{M}^{(k)}$	$\hat{\Psi}^{(k)}$	$\hat{T}^{(k)}$	$\hat{Y}^{(k)}$
Dms	a	100×100	7606	86	55.8	34.03	0.818	0.140	0.414	0.078
	b	100×100	6679	73	45.5	40.07	0.826	0.126	0.429	0.050
Dys	a	100×100	4388	118	65	27.04	0.695	0.253	0.474	0.089
	b	100×100	4065	122	62.9	25.97	0.806	0.155	0.490	0.071
	c	100×100	3132	92	73.2	30.48	0.862	0.092	0.512	0.071
	d	100×100	4302	85	87.5	36.75	0.853	0.087	0.518	0.013
Hp	a	100×100	4453	119	67.7	38.99	0.754	0.210	0.462	0.083
	b	100×100	7441	104	93.7	36.72	0.651	0.293	0.421	0.095
	c	100×100	6992	126	64.3	39.49	0.781	0.160	0.454	0.059
	d	100×100	6980	106	72.1	48.07	0.766	0.170	0.444	0.072
Jws	a	100×100	3211	94	60.5	26.15	0.753	0.207	0.491	0.101
	b	100×100	6732	96	46.1	29.03	0.712	0.253	0.399	0.111
	c	100×100	8768	103	37.8	34.73	0.668	0.285	0.369	0.107
MI	a	100×100	4320	127	65	18.68	0.643	0.324	0.448	0.093
	b	100×100	5319	134	45.8	18.18	0.699	0.270	0.472	0.090
	c	100×100	4061	133	44.5	21.01	0.713	0.235	0.476	0.058
Sws	a	100×100	8835	194	56.8	32.45	0.827	0.119	0.459	0.036
	b	100×100	6689	161	62.1	28.23	0.776	0.170	0.474	0.045
	c	100×100	6368	132	37.7	23.3	0.869	0.083	0.475	0.041
	d	100×100	8806	160	36.8	28.83	0.817	0.127	0.414	0.042
	e	100×100	8004	172	40.8	32.52	0.874	0.094	0.472	0.040
Wyl	a	300×300	7933	216	88.4	41.32	0.916	0.052	0.512	0.033

high mingling on the explanatory variable than small slope values (Dalgaard 2008).

The definition of low and high mingling is related to species richness and species abundance in forest ecosystems. Compared with boreal and temperate forests, tree species diversity is generally much higher in subtropical and tropical forests, and hence mean species mingling of trees is greater in such ecosystems. Based on the empirical probability distribution of mingling scores in these species-rich forest communities, we found that approximately 60% of all trees had mingling values of 0.75 or 1 when four neighbors were used, implying that most trees had a high proportion of heterospecific immediate neighbors. Since our objective was to compare species mingling among individual trees, a low criterion for high mingling caused identical classifications for almost all individuals. Therefore, considering the overall tree species abundances and probability distribution of mingling scores in these forest plots, we defined species mingling as high when trees had no conspecific neighbors or at least had $k - 1$ heterospecific neighbors out of their k neighboring trees (i.e., $M_i^{(k)} \geq \frac{k-1}{k}$). Then, the binary response variable

(low/high mingling) was regressed using the logistic regression analysis when $k = 4, 6, 8,$ and 10 trees were used to calculate the mingling index, respectively.

Community mingling-size relationship can also be caused by correlations between mean tree size of species population and population abundance, for example, when abundant species populations are small-sized trees, while large-sized trees may be of species that are less abundant or even rare. Therefore, with a focus on disentangling mingling-size relationships between the whole community and species levels, we also investigated size-dependent mingling effects at the level of species populations. As a reference, we present the results for the 10 most abundant species involving *Rhododendron latoucheae*, *Eurya rubiginosa* var. *attenuate*, *Camellia cuspidate*, etc., in the Wuyanling 9-ha large area plot in order to ensure sufficient sample sizes for each species, and to obtain reliable logistic regression parameters.

All analyses were performed using our own R (R Development Core Team 2019) and C++ scripts, and the packages spatstat (Baddeley et al. 2015) and Rcpp (Eddelbuettel et al. 2011) were used in our calculations.

3 Results

3.1 Forest community structure characteristics

All research plots involved high numbers of tree species ranging from 73 to 216 (Table 2), and species richness per hectare was the highest in the Sws tropical monsoon rainforest plots, reaching 194 species per hectare. Tree density ranged from 3132 in Dys c to 8835 trees per hectare in Sws a. The lowest stand basal area values were in the MI Karst forest plots varying from 18.2 to 21.0 m² ha⁻¹, while the highest values were found in Hp forest plots (36.7–48.1 m² ha⁻¹) and Wyl forest (41.3 m² ha⁻¹). Maximum diameter at breast height (dbh) was smallest in plot Sws d (36.8 cm) and largest in Wyl forest, reaching 88.4 cm.

Large species mingling values (Table 2), with most of the stands being larger than 0.7, indicated high spatial species diversity. Species segregation index ($\hat{\Psi}$) values were exclusively positive, implying conspecific aggregation in all plots; the maximum $\hat{\Psi}$ value, 0.32, was found in MI a. Size differentiation values varied between 0.37 and 0.52 indicating moderate to strong size inequality, and positive size segregation index (\hat{Y}) values across plots also indicated aggregation of trees of similar sizes.

Among the forest plots, we found that stands with lower species mingling showed size segregation (i.e., aggregation of similar tree sizes) ($\hat{Y} \sim \hat{M}$, $r = -0.78$) (Fig. 2A). Further, the strong positive relationship between species and size segregation indices shown in Fig. 2B highlights the general trend that species segregation was correlated to size segregation ($\hat{Y} \sim \hat{\Psi}$, $r = 0.82$). In addition, we also identified weak correlations of size differentiation and species

mingling indices ($\hat{T} \sim \hat{M}$, $r = 0.43$) and size differentiation and species segregation indices ($\hat{T} \sim \hat{\Psi}$, $r = -0.45$). These results of correlation analysis therefore support our expectation that spatial species and size diversity patterns are highly correlated among different plots. However, the less obvious relationships of $\hat{T} \sim \hat{M}$ or $\hat{T} \sim \hat{\Psi}$ also suggest that different aspects of diversity, e.g., size differentiation versus size segregation index, should be considered when exploring spatial relationships between species and size diversity.

3.2 Individual tree size and mingling

The logistic regression results clearly showed that tree size was related to their neighborhood species diversity. With increasing individual tree diameter, the probability that a tree had high species mingling increased. The same trend was obtained for all selected $k = 4, 6, 8,$ and 10 neighboring trees. The best regression results were achieved when $k = 4$ or 6 were used in the calculations, showing that 21 out of the 22 study plots produced positive slope parameters and 19 plots had statistically significant slope coefficients, indicating strong dependence of high mingling on tree size. Five plots (Jws c, MI a, MI c, Sws d, and Sws e) exhibited negative or non-significant slope parameters at $k = 4$ nearest neighbors were selected, which is also the maximum number of plots that yielded unsatisfactory regression results (Table 3 in the Appendix).

Generally, probability of high mingling for large trees (e.g., dbh > 30) was very high in the study plots. In some plots such as Wyl a, Sws a, Dys d, and Hp c, the logistic regression curve approached the horizontal asymptote of 1 with increasing tree diameters (Fig. 3), implying that large

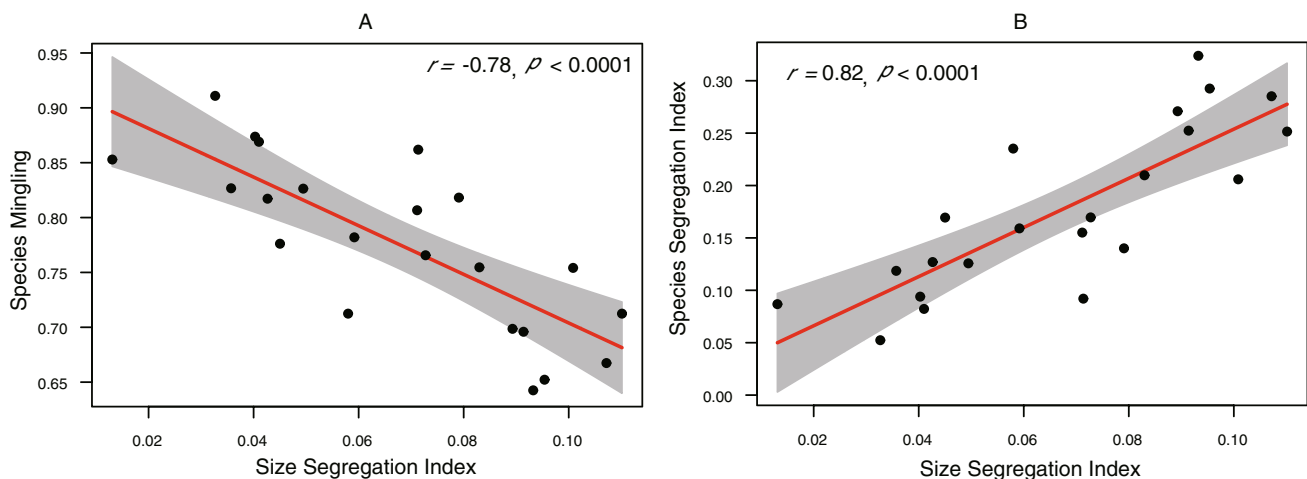


Fig. 2 Exploring the correlations of size segregation with species mingling (A) and species segregation (B) in the study plots using linear regression and 95% confidence intervals. r represents the Pearson

correlation coefficient. Four nearest neighbors were used to calculate species mingling (\hat{M}), species segregation ($\hat{\Psi}$), and size segregation indices (\hat{Y})

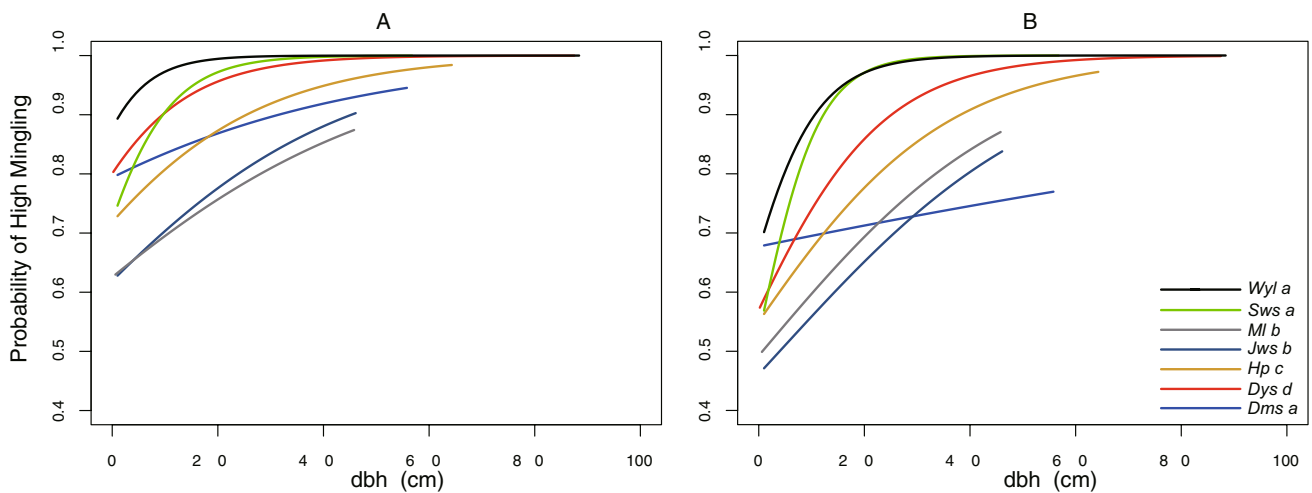


Fig. 3 Logistic regression of high species mingling with tree stem diameter (dbh) as the explanatory variable. High mingling was defined as $M_i^{(k)} \geq \frac{k-1}{k}$ when $k = 4$ (**A**) and 10 (**B**) nearest neighbors were used

trees (e.g., $\text{dbh} > 30$) were exclusively associated with high mingling scores, whereas neighborhood aggregation of conspecifics was only found for small trees, thus highlighting the strong size-dependent mingling effects.

For most of the studied species in the Wyl plot, large trees had a tendency towards high species mingling (Fig. 4), which was therefore consistent with the results at the community level. The logistic regression analysis suggested that 7–8 of the 10 species considered had positive and significant

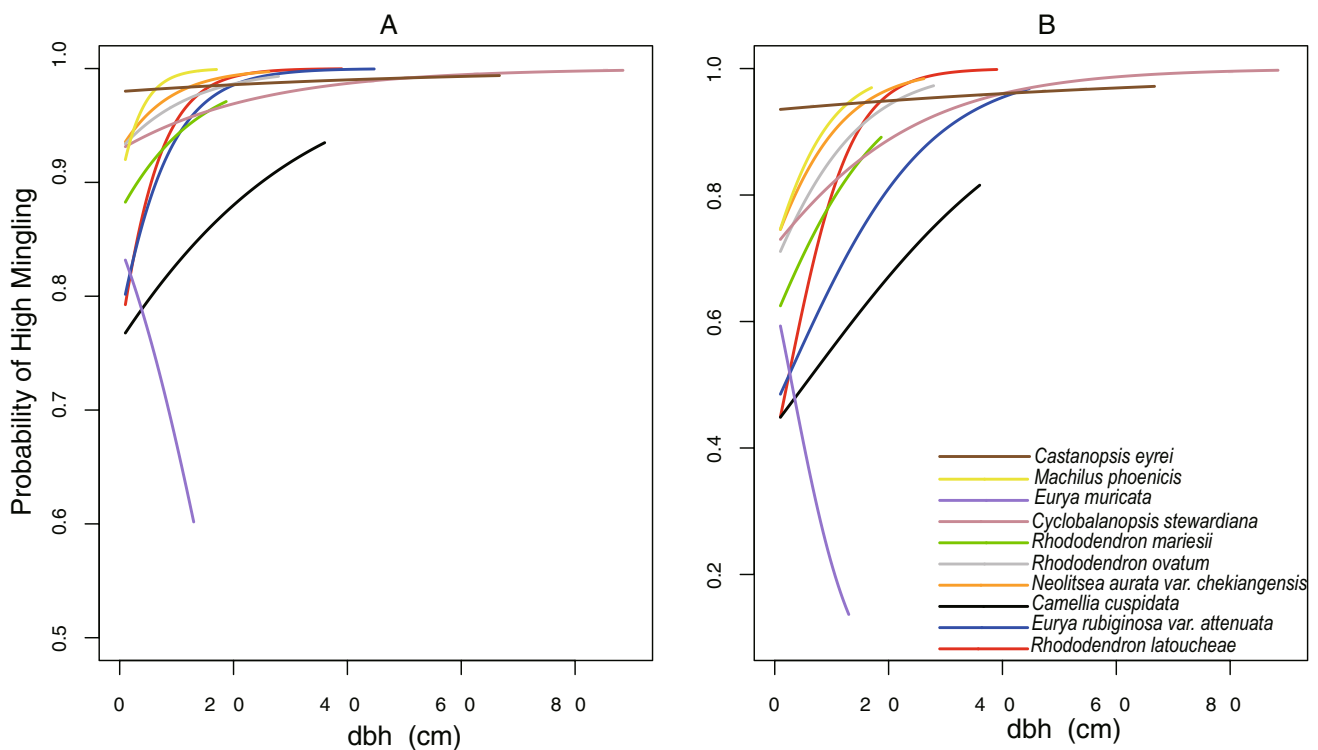


Fig. 4 Logistic regression of high mingling for the 10 most abundant species in the Wyl plot, using tree stem diameter (dbh) as the explanatory variable. High mingling was defined as $M_i^{(k)} \geq \frac{k-1}{k}$ when $k = 4$ (**A**) and 10 (**B**) nearest neighbors were used

slope regression coefficients when different k neighbors were used (Table 4 in the Appendix). Our results also revealed the general trend that the probability of high mingling approached the horizontal asymptote of 1 with increasing tree diameters whereas low mingling was associated only with small trees (Fig. 4).

3.3 Neighborhood size inequality and species mingling

Tree species mingling also increased with increasing size inequality (Fig. 5). Similar neighborhood tree sizes and thus a low local size diversity was often related to low neighborhood mingling, i.e., local neighbors of similar sizes were often from the same species.

The logistic regression results illustrated a strong relationship between spatial size and species diversity. Significant positive slope parameters ($p < 0.001$) were obtained for all selected k and in all the study plots (Table 5 in the Appendix), indicating strong dependence of high mingling on local tree size inequality. We also analyzed logistic relationships between size differentiation and species mingling for the 10 species in the large Wyl plot, and obtained similar results (not shown).

4 Discussion

Our results from the 22 species-rich natural forest communities in subtropical and tropical regions confirmed the typical relationships between spatial patterns of tree size inequality and species diversity, and therefore support the

mingling-size hypothesis. Our findings suggest that both the spatial patterns of conspecific dispersal and intra- and inter-specific interactions play an important role in determining spatial patterns of tree size and species diversity and eventually in shaping the structure of forest communities.

4.1 Intraspecific clustering and spatial structure diversity

Our plots were located in species-rich subtropical and tropical forest ecosystems with high structural variability, as indicated by the spatial species mingling and size differentiation indices. Notably, the positive values of both species and size segregation indices (Table 2) highlighted aggregated patches with individuals of the same species and with similar tree sizes in the different forest types we analyzed. Numerous studies have documented aggregated distributions among conspecifics in various vegetation types due to dispersal limitation and environmental filtering (Condit et al. 2000; Seidler and Plotkin 2006; Perry et al. 2008; Shen et al. 2013), and these processes also lead to spatial heterospecific segregation with low species mingling at close proximity (McGill 2010; Chacón-Labelle et al. 2017). Such low heterospecific mingling caused by intraspecific clustering may also result in the spatial tree size segregation (i.e., aggregation of trees with similar sizes). This can be explained by species-specific size distributions in plant communities (Pommerening et al. 2020; Wang et al. 2020): Often size inequality is the result of heterospecific mingling where different species have different size ranges and, thus, the spatial aggregation of conspecifics leads to neighborhood size segregation. Figure 6 (in the Appendix), which allows a straightforward comparison

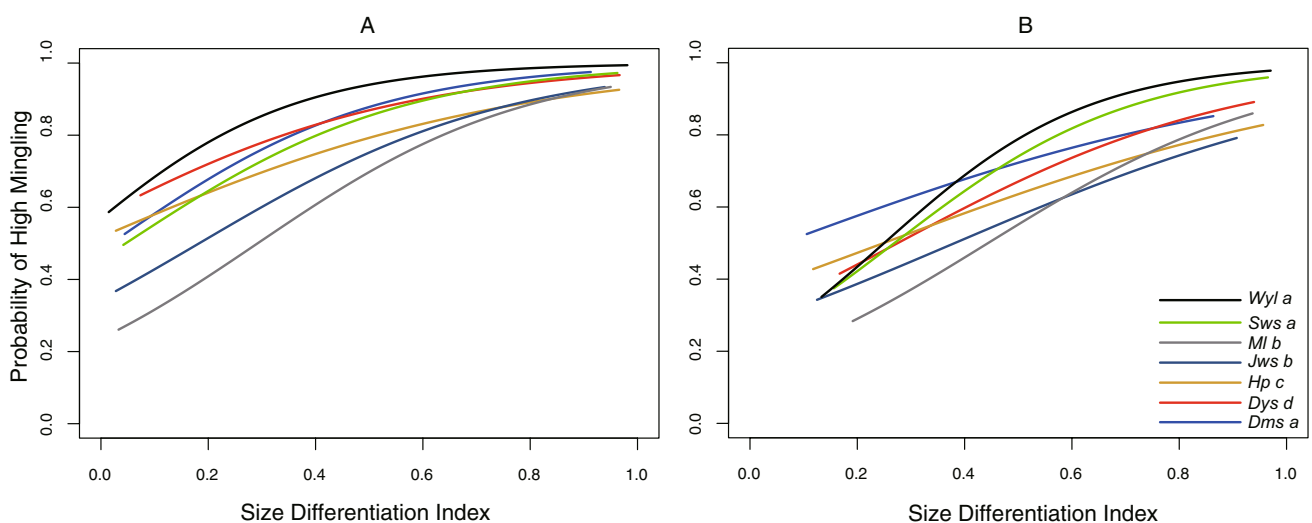


Fig. 5 Logistic regression of high species mingling using tree size differentiation ($T_i^{(k)}$) as the explanatory variable. High mingling was defined as $M_i^{(k)} \geq \frac{k-1}{k}$ when $k = 4$ (A) and 10 (B) nearest neighbors were used

of tree size (dbh) density distributions of different species, confirmed that, within a forest community, tree size distributions were distinctly different between the most dominant species while conspecific trees were often limited in a specific size range. Such ecological processes can be also indicated by the fact that the size segregation index in our study plots always had positive values, and by the significant correlations between species mingling/segregation indices and the size segregation index. Low species mingling or segregation of heterospecifics is related to segregation of trees with dissimilar sizes, thus suggesting that processes determining the clustering of conspecifics are critical in shaping spatial structural diversity in plant communities.

4.2 Size-dependent species mingling

Intraspecific clustering resulted in low mingling of individual trees whereas neighborhood species diversity differed significantly between small and large individuals. The logistic regression results across various forest communities (Table 3 in the Appendix) suggested that only small trees were found to have more conspecific neighbors in their vicinity, while large trees were exclusively associated with high species mingling, as indicated by the probabilities of high mingling approaching 1. The community-level mingling-size effects can be plausibly explained by the relationship between the stature of a species and its abundance in plant communities: Species of large size are often less abundant than small-sized species (Gaston and Spicer 2013) and therefore the expected mingling of large trees would be greater. This represents the outcome of successional processes, in which dominant and shade-intolerant species first emerge or colonize a forest, and then decrease in numbers and later are replaced by small trees of other less dominant species as succession progresses (Suzuki et al. 2008; Pommerening and Uria-Diez 2017). However, our analysis of the most abundant species in the large Wyl plot suggests that the mingling-size effects are also very typical of individual species populations, i.e., local species diversity of early-stage trees increases as they grow to become large trees. These findings confirm that localized tree interactions, JC effects and herd protection hypothesis, play important roles in driving the structure of plant communities and eventually lead to size-dependent mingling effects in various types of natural forests.

4.3 Neighborhood size differentiation and species diversity

Size-dependent mingling also implies that neighborhood size and species diversity of individual trees are significantly

correlated, as demonstrated by the results of our logistic regressions using tree size differentiation as the explanatory variable. Slope values were positive and highly significant for all plots, indicating that neighborhood species mingling is strongly dependent on its local neighborhood size differentiation. This dependence relationship is more pervasive and distinct than those obtained using dbh alone (see Tables 3 and 5 in the Appendix). Generally, large trees contribute markedly to local size differentiation, which is indicated by the positive relationships of individual dbh and size differentiation index (not shown), and they are often surrounded by neighbors of other species in their vicinity; therefore, large-sized trees strengthen both the local spatial heterogeneity of species and size structures. The association of low mingling with low size differentiation also illustrates the correlation between species richness and size variability in plant communities as reported previously (Hakkenberg et al. 2016; Pommerening et al. 2020). Because the size range is limited within a single species, aggregation of conspecifics leads to lower size diversity.

4.4 Implications for forest conservation management

Our results indicated that mingling-size effects are widespread in various types of natural forests, which has practical significance for biodiversity conservation and increasing stand structural diversity. Size-dependent mingling effects strongly support the notion that large trees have a significant contribution to the spatial structure heterogeneity in forest ecosystems (Lutz et al. 2013; Wang et al. 2018). Because large trees represent the “future” of small trees in natural forests, such effects also support the hypothesis that increasing localized mingling of individual trees is a natural outcome of forest development, which should be considered when seeking to optimize forest stand spatial structure in the context of forest management (Bettinger and Tang 2015). The significant positive relationship between tree neighborhood size variation and species diversity has another important implication for conservation and management; that is, size diversity can be enhanced when species mingling is increased in plant communities, and vice versa.

5 Conclusion

Our findings suggest that both the spatial patterns of conspecific dispersal and neighborhood interactions play an important role in determining the spatial patterns of tree size and species diversity and eventually in shaping the structure of forest communities.

Appendix

Table 3 Results of logistic regression of the probability of high species mingling using tree dbh as the explanatory variable. k denotes the number of nearest neighbors used to calculate the mingling index. High mingling was defined as $M_i^{(k)} \geq \frac{k-1}{k}$. β_1 and β_0 represent the

slope and intercept parameters in the regressions. ***/**/* indicate p values $<0.001/<0.01/<0.05$, respectively. Negative or non-significant slope parameters are bold

Forest region	Plot	$k=4$		$k=6$		$k=8$		$k=10$	
		β_1	β_0	β_1	β_0	β_1	β_0	β_1	β_0
Dms	a	0.026**	1.351	0.023**	1.075	0.016**	0.883	0.009	0.735
	b	0.031***	1.334	0.020**	1.140	0.018**	0.916	0.017**	0.728
Dys	a	0.017**	0.542	0.017**	0.335	0.018***	0.173	0.019***	0.026
	b	0.063***	1.009	0.068***	0.636	0.069***	0.410	0.061***	0.271
	c	0.017*	1.825	0.026***	1.365	0.027***	1.072	0.031***	0.815
Hp	d	0.085***	1.386	0.082***	0.896	0.087***	0.539	0.076***	0.284
	a	0.047***	0.653	0.052***	0.350	0.046***	0.195	0.043***	0.057
	b	0.044***	0.175	0.046***	-0.065	0.050***	-0.231	0.055***	-0.409
	c	0.050***	0.937	0.050***	0.632	0.052***	0.390	0.053***	0.201
Jws	d	0.024***	0.859	0.022***	0.586	0.024***	0.351	0.021***	0.185
	a	0.026***	0.810	0.023***	0.512	0.023***	0.318	0.019***	0.179
	b	0.038***	0.485	0.043***	0.201	0.042***	0.004	0.038***	-0.145
	c	-0.002	0.453	0.002	0.233	0.005	0.054	0.006	-0.080
Ml	a	0.010	0.249	0.014*	0.058	0.021**	-0.134	0.030***	-0.304
	b	0.031***	0.516	0.037***	0.273	0.039***	0.121	0.042***	-0.025
	c	0.002	0.701	0.011	0.392	0.016**	0.199	0.019**	0.025
Sws	a	0.129***	0.952	0.153***	0.558	0.172***	0.257	0.170***	0.107
	b	0.053***	0.808	0.064***	0.332	0.069***	0.043	0.070***	-0.139
	c	0.023*	1.930	0.041***	1.355	0.049***	1.013	0.052***	0.758
	d	-0.018	1.519	-0.012	1.061	-0.017**	0.810	-0.019**	0.598
	e	0.005	1.989	0.009	1.551	0.010	1.277	0.011	1.052
Wyl	a	0.161***	1.964	0.155***	1.364	0.147***	0.974	0.139***	0.714

Table 4 Results of logistic regression for the 10 most abundant species in the Wyl 9-ha plot. Probability of high species mingling was predicted using tree dbh as the explanatory variable. k denotes the number of nearest neighbors used to calculate the mingling index. High mingling was

defined as $M_i^{(k)} \geq \frac{k-1}{k}$. β_1 and β_0 represent the slope and intercept parameters in the regressions. ***/**/* indicate p values $<0.001/<0.01/<0.05$, respectively. Negative or non-significant slope parameters are bold

No	Species	$k=4$		$k=6$		$k=8$		$k=10$	
		β_1	β_0	β_1	β_0	β_1	β_0	β_1	β_0
1	<i>Rhododendron latoucheae</i>	0.189***	1.152	0.176***	0.469	0.170***	0.024	0.177***	-0.379
2	<i>Eurya rubiginosa var. attenuate</i>	0.148***	1.248	0.118***	0.615	0.114***	0.144	0.079**	-0.138
3	<i>Camellia cuspidate</i>	0.041	1.153	0.048*	0.468	0.050**	0.009	0.048**	-0.254
4	<i>Neolitsea aurata var. chekiangensis</i>	0.127**	2.549	0.115***	1.935	0.100***	1.429	0.120***	0.954
5	<i>Rhododendron ovatum</i>	0.086**	2.562	0.108***	1.694	0.096***	1.188	0.099***	0.799
6	<i>Rhododendron mariesii</i>	0.084**	1.933	0.066**	1.376	0.086***	0.782	0.090***	0.420
7	<i>Cyclobalanopsis stewardiana</i>	0.043**	2.564	0.048***	1.855	0.051***	1.374	0.056***	0.937
8	<i>Eurya muricete</i>	-0.098**	1.696	-0.139***	1.143	-0.139***	0.735	-0.184***	0.560
9	<i>Machilus phoenicis</i>	0.291**	2.151	0.229**	1.613	0.140*	1.255	0.149**	0.928
10	<i>Castanopsis eyrie</i>	0.018	3.879	0.018	3.219	0.007	3.019	0.013	2.659

Table 5 Results of logistic regression of the probability of high species mingling using tree size differentiation as the explanatory variable. k denotes the number of nearest neighbors used to calculate the mingling and size differentiation indices. High mingling was defined as $M_i^{(k)} \geq \frac{k-1}{k}$. β_1 and β_0 represent the slope and intercept parameters in the regressions. ***/**/* indicate p values $< 0.001 / < 0.01 / < 0.05$, respectively

Forest region	Plot	$k=4$		$k=6$		$k=8$		$k=10$	
		β_1	β_0	β_1	β_0	β_1	β_0	β_1	β_0
Dms	a	4.084***	-0.069	3.393***	-0.158	2.878***	-0.215	2.179***	-0.130
	b	5.482***	-0.599	4.212***	-0.466	3.781***	-0.560	3.020***	-0.454
Dys	a	3.766***	-1.075	3.512***	-1.226	3.194***	-1.259	3.004***	-1.328
	b	3.419***	-0.271	3.549***	-0.730	3.891***	-1.133	4.051***	-1.404
	c	3.377***	0.321	3.207***	-0.046	2.727***	-0.115	2.856***	-0.427
	d	3.200***	0.283	3.284***	-0.281	3.388***	-0.673	3.121***	-0.854
Hp	a	4.005***	-0.774	4.100***	-1.154	3.903***	-1.283	3.697***	-1.364
	b	3.523***	-1.051	3.465***	-1.306	3.260***	-1.388	3.299***	-1.579
	c	2.460***	0.107	2.343***	-0.170	2.224***	-0.362	2.238***	-0.561
	d	2.351***	-0.010	1.992***	-0.169	2.120***	-0.460	2.083***	-0.634
Jws	a	2.825***	-0.361	3.161***	-0.863	2.997***	-1.005	2.827***	-1.097
	b	3.549***	-0.653	3.090***	-0.778	2.756***	-0.866	2.509***	-0.950
	c	3.577***	-0.844	3.187***	-0.948	2.666***	-0.935	2.336***	-0.951
MI	a	4.029***	-1.468	3.685***	-1.564	3.474***	-1.642	3.294***	-1.692
	b	3.971***	-1.149	3.650***	-1.291	3.710***	-1.493	3.695***	-1.636
	c	2.693***	-0.530	2.587***	-0.772	2.556***	-0.942	2.446***	-1.058
Sws	a	3.796***	-0.140	3.983***	-0.561	4.148***	-0.884	4.501***	-1.208
	b	4.179***	-0.802	3.952***	-1.173	3.901***	-1.434	4.079***	-1.703
	c	2.181***	1.051	2.363***	0.458	2.735***	-0.027	2.724***	-0.273
	d	3.182***	0.170	2.741***	-0.115	2.618***	-0.352	2.546***	-0.557
	e	2.466***	0.903	2.519***	0.443	2.519***	0.160	2.604***	-0.107
Wyl	a	4.942***	0.279	5.157***	-0.508	5.211***	-0.983	5.272***	-1.319

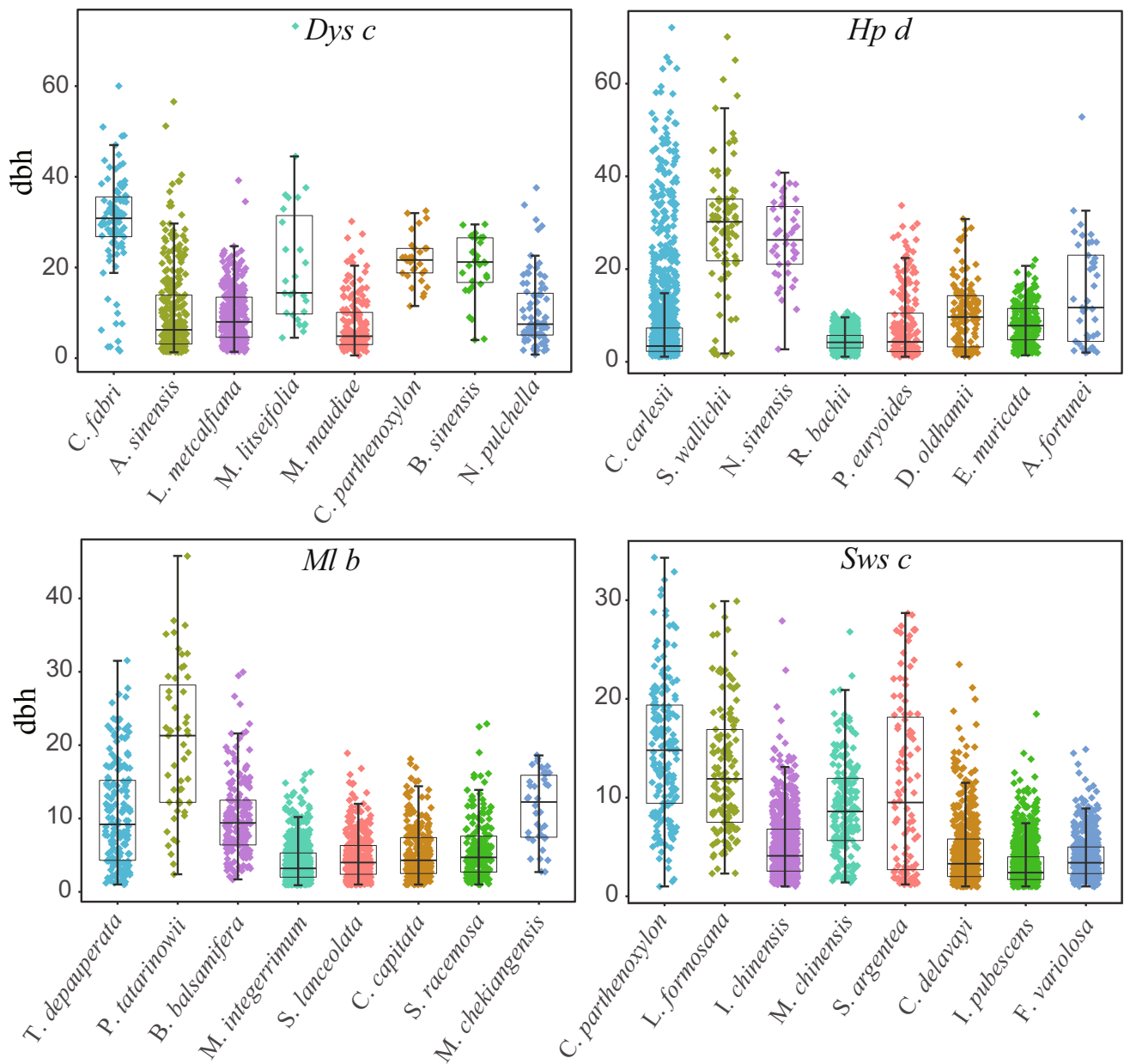


Fig. 6 Boxplots characterizing tree dbh size distributions of the most dominant species (in terms of basal area) in the research plots Dys c, Hp d, MI b, and Sws c

Acknowledgements We express our gratitude to our colleagues who contributed to the establishment of the forest plots involved in this study.

Author contribution H. W. and K. C. designed the research and the experiments. H. W., S. H., and H. P. analyzed the data, programmed, and prepared the results. K. C. and S. Z. were involved in the data collection, and contributed to the interpretation of the results. H. W. and K. C. wrote the manuscript and all authors were involved in the discussion of the results.

Funding This research was supported by the National Key Research and Development Program of China (project no. 2016YFC0502101-04)

and the Guangxi Key Research and Development Program (project no. AB16380254).

Data availability The datasets generated and/or analyzed during the current study are deposited at Dryad, <https://doi.org/10.5061/dryad.8cz8w9gr3>

Code availability The programming code used for the current study is available from the authors on request.

Declarations

Ethics approval Not applicable.

Consent to participate Not applicable.

Consent for publication. All authors gave their informed consent to this publication and its content.

Conflict of interest The authors declare no competing interests.

References

- Aguirre O, Hui G, von Gadow K, Jiménez J (2003) An analysis of spatial forest structure using neighbourhood-based variables. *For Ecol Manage* 183:137–145
- Armas C, Pugnaire FI (2005) Plant interactions govern population dynamics in a semi-arid plant community. *J Ecol* 93:978–989
- Baddeley A, Rubak E, Turner R (2015) Spatial point patterns: methodology and applications with R. CRC Press
- Bagchi R, Henrys PA, Brown PE, Burslem DF, Diggle PJ, Gunatilleke CV et al (2011) Spatial patterns reveal negative density dependence and habitat associations in tropical trees. *Ecology* 92:1723–1729
- Bettinger P, Tang M (2015) Tree-level harvest optimization for structure-based forest management based on the species mingling index. *Forests* 6:1121–1144
- Brown JH, Mehlman DW, Stevens GC (1995) Spatial variation in abundance. *Ecology* 76:2028–2043
- Chacón-Labela J, de la Cruz M, Escudero A (2017) Evidence for a stochastic geometry of biodiversity: the effects of species abundance, richness and intraspecific clustering. *J Ecol* 105:382–390
- Chesson P (2000) Mechanisms of maintenance of species diversity. *Annu Rev Ecol Syst* 31:343–366
- Condit R, Ashton PS, Baker P, Bunyavejchewin S, Gunatilleke S, Gunatilleke N et al (2000) Spatial patterns in the distribution of tropical tree species. *Science* 288:1414–1418
- Connell J (1970) On the role of natural enemies in preventing competitive exclusion in some marine animals and in rain forest trees. In: Den Boer PJ, & Gradwell GR (Eds.), *Dynamics of populations*, pp 298–312
- Dalgaard P (2008) *Introductory statistics with R*. Springer
- Dyer LA, Singer M, Lill J, Stireman J, Gentry G, Marquis RJ et al (2007) Host specificity of Lepidoptera in tropical and temperate forests. *Nature* 448:696–699
- Eddelbuettel D, François R, Allaire J, Ushey K, Kou Q, Russel N et al (2011) Rcpp: seamless R and C++ integration. *J Stat Softw* 40(8):1–18
- Forister ML, Novotny V, Panorska AK, Baje L, Basset Y, Butterill PT et al (2015) The global distribution of diet breadth in insect herbivores. *Proc Natl Acad Sci* 112:442–447
- Gadow KV, Fuldner K (1993) Zur bestandesbeschreibung in der forsteinrichtung. *Forst Und Holz* 48:602–606
- Gadow KV, Zhang CY, Wehenkel C, Pommerening A, Corral-Rivas J, Korol M, Myklush S, Hui GY, Kiviste A, Zhao XH (2012) Forest structure and diversity. In: *Continuous Cover Forestry*. Springer, Dordrecht, pp 29–83
- Gaston KJ, Spicer JI (2013) *Biodiversity: an introduction*. John Wiley, Sons
- Germany MS, Bruehlheide H, Erfmeier A (2019) Janzen-Connell effects in a forest BEF experiment: strong distance-dependent seedling establishment of multiple species. *Ecology* 100:e02736
- Hakkenberg CR, Song C, Peet RK, White PS (2016) Forest structure as a predictor of tree species diversity in the North Carolina Piedmont. *J Veg Sci* 27:1151–1163
- Hui G, Pommerening A (2014) Analysing tree species and size diversity patterns in multi-species uneven-aged forests of Northern China. *For Ecol Manage* 316:125–138
- Huston M (1979) A general hypothesis of species diversity. *Am Nat* 113:81–101
- Janzen DH (1970) Herbivores and the number of tree species in tropical forests. *Am Nat* 104: 501–528
- LaManna JA, Mangan SA, Alonso A, Bourg NA, Brockelman WY, Bunyavejchewin S et al (2017) Plant diversity increases with the strength of negative density dependence at the global scale. *Science* 356:1389–1392
- Levine JM, Bascompte J, Adler PB, Allesina S (2017) Beyond pairwise mechanisms of species coexistence in complex communities. *Nature* 546:56–64
- Liang J, Buongiorno J, Monserud RA, Kruger EL, Zhou M (2007) Effects of diversity of tree species and size on forest basal area growth, recruitment, and mortality. *For Ecol Manage* 243:116–127
- Lutz JA, Larson AJ, Freund JA, Swanson ME, Bible KJ (2013) The importance of large-diameter trees to forest structural heterogeneity. *PLoS one* 8(12):e82784
- McGill BJ (2010) Towards a unification of unified theories of biodiversity. *Ecol Lett* 13:627–642
- Perry G, Enright N, Miller B, Lamont B (2008) Spatial patterns in species-rich sclerophyll shrublands of southwestern Australia. *J Veg Sci* 19:705–716
- Peters HA (2003) Neighbour-regulated mortality: the influence of positive and negative density dependence on tree populations in species-rich tropical forests. *Ecol Lett* 6:757–765
- Pommerening A, Grabarnik P (2019) *Individual-based methods in forest ecology and management*. Springer
- Pommerening A, Svensson A, Zhao Z, Wang H, Myllymäki M (2019) Spatial species diversity in temperate species-rich forest ecosystems: revisiting and extending the concept of spatial species mingling. *Ecol Ind* 105:116–125
- Pommerening A, Uria-Diez J (2017) Do large forest trees tend towards high species mingling? *Eco Inform* 42:139–147
- Pommerening A, Wang H, Zhao Z (2020) Global woodland structure from local interactions: new nearest-neighbour functions for understanding the ontogenesis of global forest structure. *Forest Ecosystems* 7:1–11
- Pretzsch H (2009) *Forest dynamics, growth and yield: from measurement to model*. Springer Verlag, Berlin Heidelberg
- Raventós J, Wiegand T, Luis MD (2010) Evidence for the spatial segregation hypothesis: a test with nine-year survivorship data in a Mediterranean shrubland. *Ecology* 91:2110–2120
- Seidler TG, Plotkin JB (2006) Seed dispersal and spatial pattern in tropical trees. *PLoS Biology* 4:e344
- Shen G, He F, Waagepetersen R, Sun I, Hao Z, Chen Z-S et al (2013) Quantifying effects of habitat heterogeneity and other clustering processes on spatial distributions of tree species. *Ecology* 94:2436–2443
- Shuai F, Wang Y, Yu S (2014) Density dependence in forests is stronger in tropical and subtropical climates among closely related species. *Ecography* 37:659–669
- Sterner RW, Ribic CA, Schatz GE (1986) Testing for life historical changes in spatial patterns of four tropical tree species. *J Ecol* 74:621–633
- Suzuki SN, Kachi N, Suzuki J (2008) Development of a local size hierarchy causes regular spacing of trees in an even-aged Abies forest: analyses using spatial autocorrelation and the mark correlation function. *Ann Bot* 102(3):435–441
- R Core Team (2019) *R: A language and environment for statistical computing*. Vienna, Austria: R Foundation for Statistical Computing. URL: <https://www.R-project.org>. Accessed 18 June 2019

- Wang H, Peng H, Hui G, Hu Y, Zhao Z (2018) Large trees are surrounded by more heterospecific neighboring trees in Korean pine broad-leaved natural forests. *Sci Rep* 8:1–11
- Wang H, Zhao Z, Myllymäki M, Pommerening A (2020) Spatial size diversity in natural and planted forest ecosystems: revisiting and extending the concept of spatial size inequality. *Ecological Informatics* 57:101054
- Wang Hongxiang et al (2021) Data from: Localized neighborhood species mingling is correlated with individual tree size inequality in natural forests in South China. , Dryad repository, V1. <https://doi.org/10.5061/dryad.8cz8w9gr3>
- Wen Y, Yuan C, Li X, He T, Lai J, Huang M (1998) Development of species diversity in vegetation restoration process in mid-mountain region of Damingshan, Guangxi. *Acta Phytocologica Sinica* 22: 33–40
- Wills C, Condit R, Foster RB, Hubbell SP (1997) Strong density-and diversity-related effects help to maintain tree species diversity in a neotropical forest. *Proc Natl Acad Sci* 94:1252–1257
- Wright JS (2002) Plant diversity in tropical forests: a review of mechanisms of species coexistence. *Oecologia* 130:1–14
- Yao J, Zhang X, Zhang C, Zhao X, von Gadow K (2016) Effects of density dependence in a temperate forest in northeastern China. *Sci Rep* 6(1):1–11
- Zhong L, Chang-Yang C, Lu P, Gu X, Lei Z, Cai Y et al (2015) Community structure and species composition of the secondary evergreen broad-leaved forest: the analyses for a 9 ha forest dynamics plot in Wuyanling Nature Reserve, Zhejiang Province, East China. *Biodiversity Science* 23:619–629
- Zhu Y, Mi X, Ren H, Ma K (2010) Density dependence is prevalent in a heterogeneous subtropical forest. *Oikos* 119:109–119

Publisher's Note Springer Nature remains neutral with regard to jurisdictional claims in published maps and institutional affiliations.